Collective excitations in a dense dipolar fluid studied by inelastic neutron scattering

1991 J. Phys.: Condens. Matter 3 4075

(http://iopscience.iop.org/0953-8984/3/22/017)

J. Phys.: Condens. Matter 3 (1991) 4075–4087. Printed in the UK

Collective excitations in a dense dipolar fluid studied by inelastic neutron scattering

J L Martínez†, F J Bermejo‡, M García-Hernández§, F J Mompeán§, E Enciso‖ and D Martín‡

† Institut Laue–Langevin, 156X, F-38042 Grenoble Cédex, France
‡ Instituto de Estructura de la Materia, CSIC, Serrano 119, E-28006 Madrid, Spain
§ ISIS Pulsed Neutron Facility, Rutherford Appleton Laboratory, Chilton, Didcot, Oxon OX11 0QX, UK
‖ Departamento de Química-Física, Facultad de Ciencias Químicas, Universidad Complutense, E-28040 Madrid, Spain

Received 3 December 1990, in final form 18 February 1991

Abstract. The inelastic neutron scattering spectra of liquid sulphur dioxide have been measured for two thermodynamic states and for the momentum-transfer range $0.35 \leqslant Q \leqslant 2$ Å^{-1}. The spectra show noticeable inelastic intensities, indicating the presence of propagating modes for $Q \leqslant 0.45$ Å^{-1} at $T = 266$ K and for $Q < 0.70$ Å^{-1} at $T = 210$ K. The spectra have been analysed following two different approaches: on the one hand, the underlying $S(Q, \omega)$ dynamic structure factor has been reconstructed by means of a deconvolution technique; and, on the other hand, the measured intensities are analysed on the basis of a simplified model folded with the instrumental resolution. The 'dispersion relations' obtained are finally discussed in relation to recent theoretical predictions.

1. Introduction

The collective-dynamical properties of highly polar liquids are expected to show rather distinctive features as compared with those exhibited by simpler systems, such as those formed by Lennard-Jones particles (liquified rare gases), liquid metals or model (hard-spheres) systems [1], where the interaction potentials are of short-range nature. The strong electrostatic interactions give rise in the former case to long-range strongly anisotropic forces which introduce the presence of strong orientational correlations. The possibility of observing some effects caused by the collective excitation of the polarization function (termed dipolaronic modes in close analogy with the plasmon modes in Coulomb systems) has been predicted some time ago [2] and has been re-examined in recent times [3].

In this work, the collective properties of liquid sulphur dioxide are studied by means of inelastic, triple-axis neutron spectroscopy. This type of liquid was chosen for the following reasons: (i) it constitutes an optimal representative for this class of liquids due to its low melting point and relatively simple molecular structure—the liquid structure is well known from a recent neutron diffraction study [4], where it was shown that the range of strong orientational correlations (coherent length) extends up to 20 Å; and

(ii) it is a nearly pure coherent scatterer for neutrons, a fact that will provide good counting statistics, nearly free from incoherent contributions.

The purposes of the present work are twofold: on the one hand, to provide 'dispersion relations' for this class of fluids, which are not known up to the present moment; and, on the other hand, to try to detect any effect caused by collective polarization excitations that may affect the dispersion of the observed frequencies.

The outline of the paper is as follows: the experimental and data treatment details will be presented in section 2. The interpretation of the observed spectra as well as their momentum-transfer and temperature dependences will be described in section 3. A discussion of the results is given in section 4 and, finally, section 5 contains the main conclusions.

2. Experiments and data analysis

The experiments were performed using the triple-axis spectrometer IN8 at the Institut Laue–Langevin, Grenoble (France) [5]. The useful kinematic region for this class of experiments involves the transfer of rather high energy for low Q-values (near the direct beam), so a very restrictive collimation has to be used (30′ in pile, 20′ between monochromator and sample, 10′ between sample and analyser and 40′ between analyser and detector). A cylindrical vacuum tank 1 m diameter was used to reduce the contribution coming from the diffuse scattering from the air. Most of the scans were performed on constant-Q mode with a fixed incident wavevector of 4.1 Å^{-1} with the spectrometer in the 'W' (1, −1, 1) configuration, although some spectra were also tested using the constant-k_F mode.

The monochromator and analyser used the (002) reflection of pyrolitic graphite, and the momentum-transfer range covered the region $0.35 \leqslant Q \leqslant 2\ \text{Å}^{-1}$. Both energy gain and loss sides were measured for all spectra, and the measurement temperatures were 210 K and 266 K, just above the melting point and below the boiling point, respectively.

The container followed a design previously used for other liquid samples [6, 7], and was modified to allow the in-cell condensation of room temperature gas. Such a design has been shown to reduce to a minimum the multiple-scattering contribution since the beam is partly collimated by the cadmium-coated spacers. Several runs were carried out using the empty cell which scatters less than 1% of the total intensity, and an absorption correction procedure was employed [8] to subtract the contribution of the empty container.

The instrumental resolution was also measured using a vanadium standard, which gave a width of about 0.40 THz at half width at half maximum (HWHM). Moreover, the resolution function was computed for each energy-transfer value using a code [9] based on the Cooper–Nathans formulation, and several graphs depicting the energy resolution versus energy transfer at different Q-values are shown in figure 1. The energy resolution is calculated as the expected width for the standard vanadium, at the corresponding values of Q and energy transfer [9].

A set of measured spectra for both temperatures is shown in figure 2. The full curves correspond to fits made using a model scattering law that makes use of the viscoelastic approximation [6, 7, 10] and has been shown to provide reliable results when analysing triple-axis spectra [6, 7]. Such a model scattering law is constructed as a sum of single-particle (molecular rotations and translations) and collective responses, with an amplitude governed by the structure factor for molecular centres $S_{cm}(Q)$, and a Debye–Waller

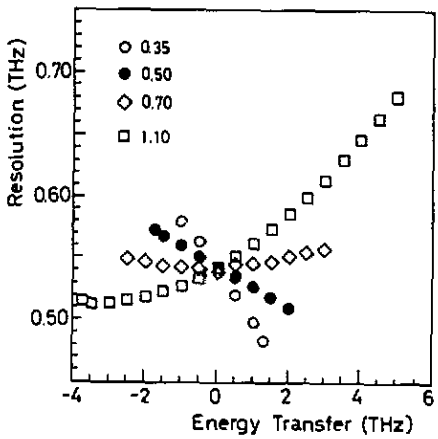

Figure 1. Energy-transfer dependence of the attainable energy resolution for different Q-values (0.35, 0.5, 0.7 and 1.1 Å^{-1}).

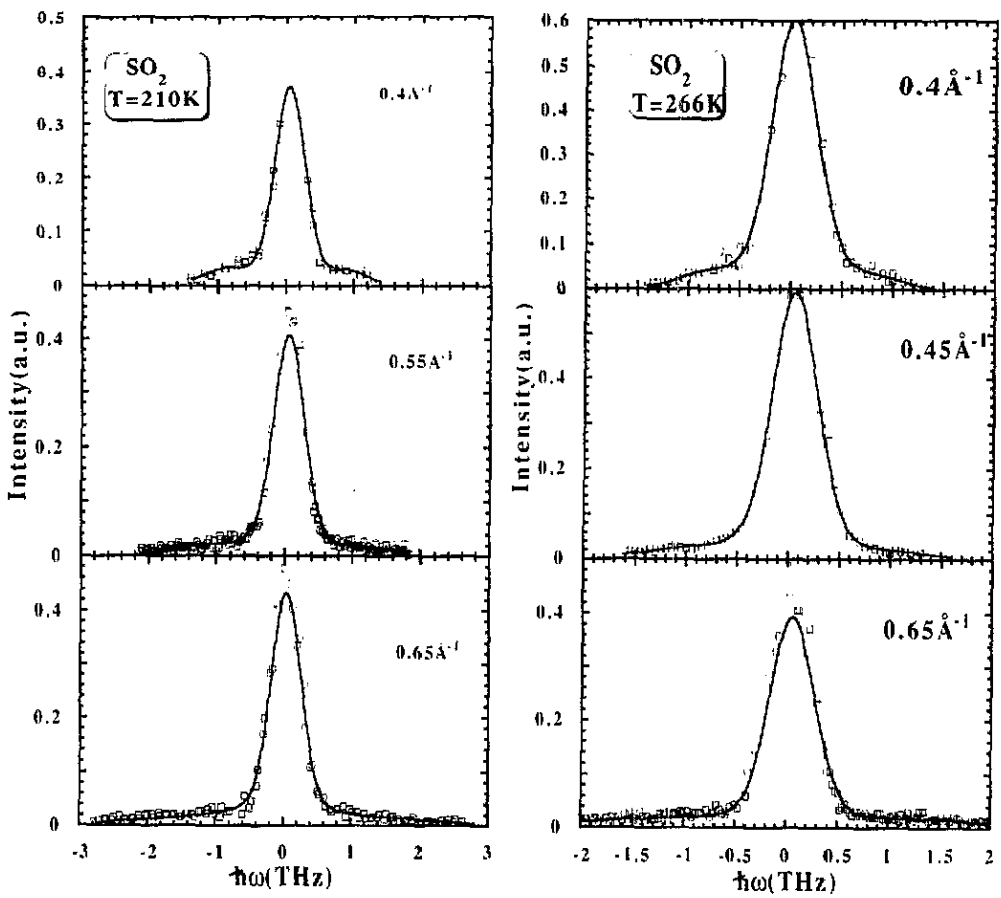

Figure 2. Corrected spectra for selected momentum-transfer values. Open squares represent experimental intensities and the full curves are fits to model functions. (*a*) T = 210 K and (*b*) T = 266 K.

term with a mean square amplitude $\langle u^2 \rangle$ set to values derived from a previous diffraction experiment [4], where the values of the mean squared amplitudes of vibration had been evaluated from a molecular force field. A value for $\langle u^2 \rangle$ was calculated as a weighted average of the self-terms (see equations (A31) and (A32) of [4]), and used as a constant in the fitting procedures. The single-particle dynamical structure factor $S_{\mathrm{qel}}(Q, \omega)$ has been modelled under the quasielastic approximation as described below, and the collective dynamics is comprised by the second, ω_0, and fourth, ω_l, frequency moments of the coherent response as well as by a relaxation time τ. The model scattering law then reads

$$S_{\mathrm{mod}}(Q, \omega) = S_{\mathrm{cm}}(Q) \exp(-\langle u^2 \rangle Q^2) \frac{1}{1 - \exp(-\hbar\omega\beta)} \times \left(S_{\mathrm{qel}}(Q, \omega) + \frac{\omega_0^2(\omega_l^2 - \omega_0^2)\tau}{[\omega\tau(\omega^2 - \omega_l^2)]^2 + (\omega^2 - \omega_0^2)^2} \right) \tag{1}$$

where $\beta = 1/k_B T$ and the relaxation time is defined using the usual approximation [10]

$$\tau^{-1} = 2[(\omega_l^2 - \omega_0^2)/\pi]^{1/2} \tag{2}$$

and the functions ω_0 and ω_l are both implicitly dependent on Q, and are considered as adjustable parameters.

The quasielastic (single-particle) response was modelled assuming a rotational diffusion law for the molecular reorientational motions, and an approximation for coherent motions was used following the lines used in previous work [6, 7], which reads

$$S_{\mathrm{qel}}(Q, \omega) = S_{l=0}(Q, \omega) + S_{l\neq 0}(Q, \omega)$$

with

$$S_{l=0}(Q, \omega) = f_{\mathrm{coh}}^2(Q)\, \Gamma_Q^* / [\omega^2 + (\Gamma_Q^*)^2]$$

where the $f(Q)$ are the molecular form factors:

$$f_{\mathrm{coh}}^2(Q) = (b_S j_0(Q r_S) + 2 b_O j_0(Q r_O))^2$$

defined in terms of scattering lengths b_v and geometrical parameters (r_v = distances to the centre of mass) given in [4]. The widths of the coherent translational component Γ_Q^* were computed using the Skold approximation, with a diffusion coefficient D_T which has been estimated from the only available molecular dynamics simulation [11], since no experimental data were found in the literature. The interpolated values were $D_T = 0.075$ Å^2 ps^{-1} at $T = 210$ K and $D_T = 0.28$ Å^2 ps^{-1} for $T = 266$ K. The rotational component was computed under the assumption of rotational diffusion:

$$S_{l\neq 0}(Q, \omega) = \sum_{l=1}^{\infty} (2l + 1) A_l^2(Q) \frac{\Gamma_l'}{\omega^2 + (\Gamma_l')^2}$$

where the form factors $A_l(Q)$ are defined in the usual way:

$$A_l^2(Q) = \sum_{v, v'=1}^{3} b_v b_{v'} j_l(Q r_v) j_l(Q r_{v'}) P_l(\cos \theta_{vv'})$$

in terms of scattering lengths, distances to the centre of mass, r, and the angle defined by the vectors joining the nuclei positions with the centre of mass, $\theta_{vv'}$ (see [4]). The

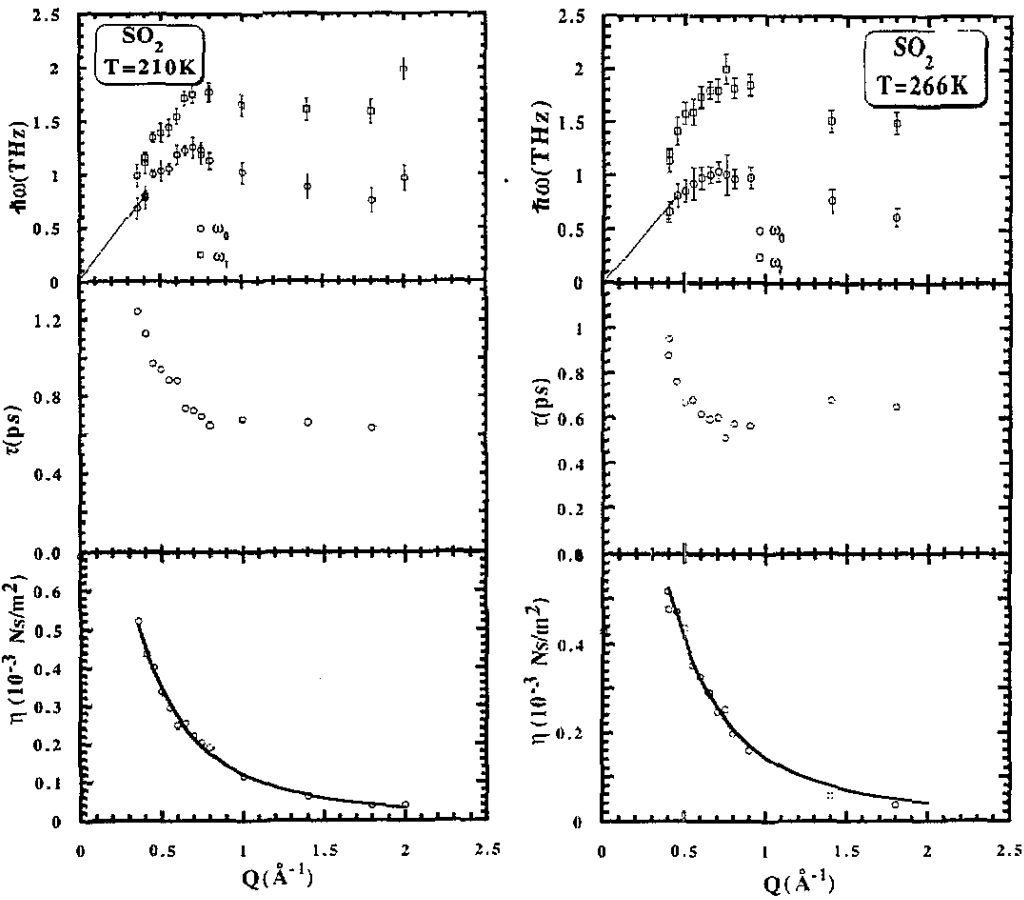

Figure 3. (*a*) Wavevector dependence of the square roots of the second and fourth frequency moments of $S(Q, \omega)$ (upper frame), relaxation times (middle frame) and longitudinal viscosity (lower frame) for $T = 210$ K. (*b*) As (*a*), but for $T = 266$ K. The full curve in the lower frame corresponds to fits made using (5). The lines in the upper frames show the extrapolation to the origin (from small Q-values) made in order to calculate the sound velocity.

widths Γ_l^1 are given under the simple rotational diffusion assumptions in terms of the rotational constant D_r:

$$\Gamma_l^1 = l(l+1)D_r + D_T Q^2$$

which is related to the usual rotational correlation time via $1/\tau_c = 6D_r$.

The estimates for the rotational constant were set to the experimental values measured by means of ^{33}S NMR [12] which were found to be in reasonable agreement with those estimated by means of a hydrodynamic approximation based on the Hu–Zwanzig model [13]. The values for the rotational correlation time were $\tau_c = 0.95 \pm 0.05$ ps and 0.41 ± 0.03 ps for $T = 210$ K and $T = 266$ K, respectively.

The model is thus completely specified by three adjustable parameters, which are the frequency moments ω_0 and ω_l and a global scale factor (normalization constant). The present treatment could be extended in order to account for the strong orientational

effects by means of an additional relaxation time. However, previous experience with other liquids [6] has shown that the simplified viscoelastic approximation given by (1) is able to take into account the most relevant features of the collective dynamics in the range of momentum transfer where the effects of the molecular shape are small (for Q-values not far beyond the first peak in the static structure factor).

The model to be compared with the experimental data is therefore

$$I(Q, \omega) = S_{\text{mod}}(Q, \omega) \otimes R(\omega) \tag{3}$$

where the symbol $\otimes$ stands for the convolution operation and $R(\omega)$ is the resolution function measured experimentally.

In order to obtain model-free estimates of the underlying $S(Q, \omega)$, a deconvolution procedure described previously [6] has been employed. The estimated dynamic structure factors were then used in order to contrast the validities of the model functions employed.

3. Results

A set of representative spectra for both temperatures is shown in figure 2. As can be seen, some disagreements are noticeable in the region near the elastic ($h\omega = 0$) value. The fits could easily be improved by introducing more refined models to treat the coherent interference effects on the single-particle dynamics, or by increasing the number of adjustable parameters. However, since the instrumental resolution achieved in this study is too low for us to discriminate between some of the currently employed models, and since it would imply an increase in the number of free parameters (for an application to the case of a mostly coherent scatterer see [14]), no attempt was made to improve the fits. The square roots of the normalized second and fourth frequency moments of the dynamic structure factor computed from the model fits, as well as the derived relaxation times and the wavevector-dependent longitudinal viscosity defined as

$$\eta_l(Q, 0) = (nM/Q^2)(\omega_l^2 - \omega_0^2)\tau \tag{4}$$

where nM represents a mass density, are shown in figures 3(a) and 3(b) for the two measured temperatures, respectively.

As can be seen from figure 3, the low-Q parts of the $\omega_0(Q)$ functions show a quasilinear behaviour from which the isothermal sound velocity v_t (related to the adiabatic velocity $v_0 = \gamma v_t$, γ being the ratio of specific heats) can be obtained. The values for the sound velocity were 1234 ± 76 m s^{-1} for $T = 210$ K and 1142 ± 89 m s^{-1} for $T = 266$ K. In both cases the $\omega_0(Q)$ curves show a maximum located about 0.7 Å^{-1} and a broad minimum located at about Q_p (the maximum of the static structure factor, which occurs at $Q \simeq 1.8$ Å^{-1}).

The computed relaxation times show a smooth behaviour with momentum transfer, with an oscillation maximum located about Q_p. Their numerical values vary within ranges from 0.64 to 1.24 ps for $T = 210$ K and from 0.56 to 0.95 ps for $T = 266$ K, thus indicating that the increase in temperature leads to an increase in the damping, and so the crossover to the overdamped regime is shifted to lower wavevectors as the temperature is increased.

The values obtained for the longitudinal viscosity $\eta_l(Q, 0)$ can be fitted using a simple expression following Alley *et al* [15]:

$$\eta_l(Q,0)^{-1} = \eta_l(0)^{-1} + B(Q/Q_c)^2 \tag{5}$$

where Q_c can be interpreted as a 'critical' Q-value corresponding to the transition to an overdamped regime, and $\eta_l(0)$ is the asymptotic value of this viscosity in the $Q \to 0$ limit. The fitted values of the three parameters ($\eta_l(0)$, B and Q) were $0.94 \pm 0.2 \times 10^{-3}$ N s m^{-2}, 10.6 ± 1.7 and 1.2 ± 0.3 Å^{-1} for $T = 210$ K and $0.89 \pm 0.14 \times 10^{-3}$ N s m^{-2}, 6.1 ± 1.1 and 0.9 ± 0.2 Å^{-1} for $T = 266$ K. We defer further discussion of this to the next section.

The values of the elastic constants ($B + \frac{4}{3}G$) can be estimated from the low-Q part of the $\omega_l(Q)$ functions since

$$\lim_{Q \to 0} \omega_l^2(Q) = \frac{Q^2}{nM}\left(B + \frac{4}{3}G\right) \tag{6}$$

where the symbols retain their usual meaning. The values for the estimated sum of elastic moduli were $0.224 \pm 0.006 \times 10^{-1}$ and $0.201 \pm 0.004 \times 10^{-1}$ N m^{-2} for the two temperatures, respectively.

In order to rationalize the dispersion of the ω_0, a simplified model initially developed by Bhatia and Singh [16] has been used. For such a purpose, the ω_0 curves were assumed to represent an effective moment, and thus they represent a sum of longitudinal and transverse components:

$$\omega_0^{-3} = \tfrac{1}{3}(\omega_{\text{long}}^{-3} + 2\omega_{\text{trans}}^{-3}) \tag{7a}$$

where

$$\omega_{\text{long}} = (1/\rho)[(2\nu\delta/a^2)(F_2 - \tfrac{1}{5}F_0)]^{1/2}F_m \tag{7b}$$

$$\omega_{\text{trans}} = (1/\rho)[(\nu\delta/a^2)(\tfrac{3}{5}F_0 - F_2)]^{1/2}F_m \tag{7c}$$

where the symbol ρ stands for the measured density [4], ν is the number of nearest neighbours, and δ is related to the second derivative of the interparticle potential at $r = a$, where a is a contact distance and F_0 and F_2 are form factors given by

$$F_0 = 1 - (\sin(Qa))/Qa \qquad F_2 = \tfrac{1}{3} - \sin(Qa)[1/Qa - 2/(Qa)^3]\,2\cos(Qa)/(Qa)^2 \tag{7d}$$

and F_m is a molecular form factor given by

$$F_m = \left(\sum_{v=1}^{3} b_v j_0(Qr_v)\Big/\sum_{v=1}^{3} b_v\right)^2$$

where the geometrical parameters are distances to the centre of mass.

Such a simplified model fits the ω_0-functions adequately up to $Q = 1.0$ Å^{-1}, and the parameters obtained are for the $T = 210$ K and $T = 266$ K measurements: $a = 3.4 \pm 0.3$ and 3.7 ± 0.2 Å^{-1}; $\nu = 29 \pm 3$ and 28 ± 1 particles; $\delta = 0.50 \pm 0.12$ and 0.35 ± 0.09 J m^{-3}, respectively.

The values obtained for the contact distance are in excellent agreement with the position of the first peak in the $g(r)$ pair distribution function determined in a recent experiment [4], and the estimated numbers of neighbours are also in agreement with the available structural data.

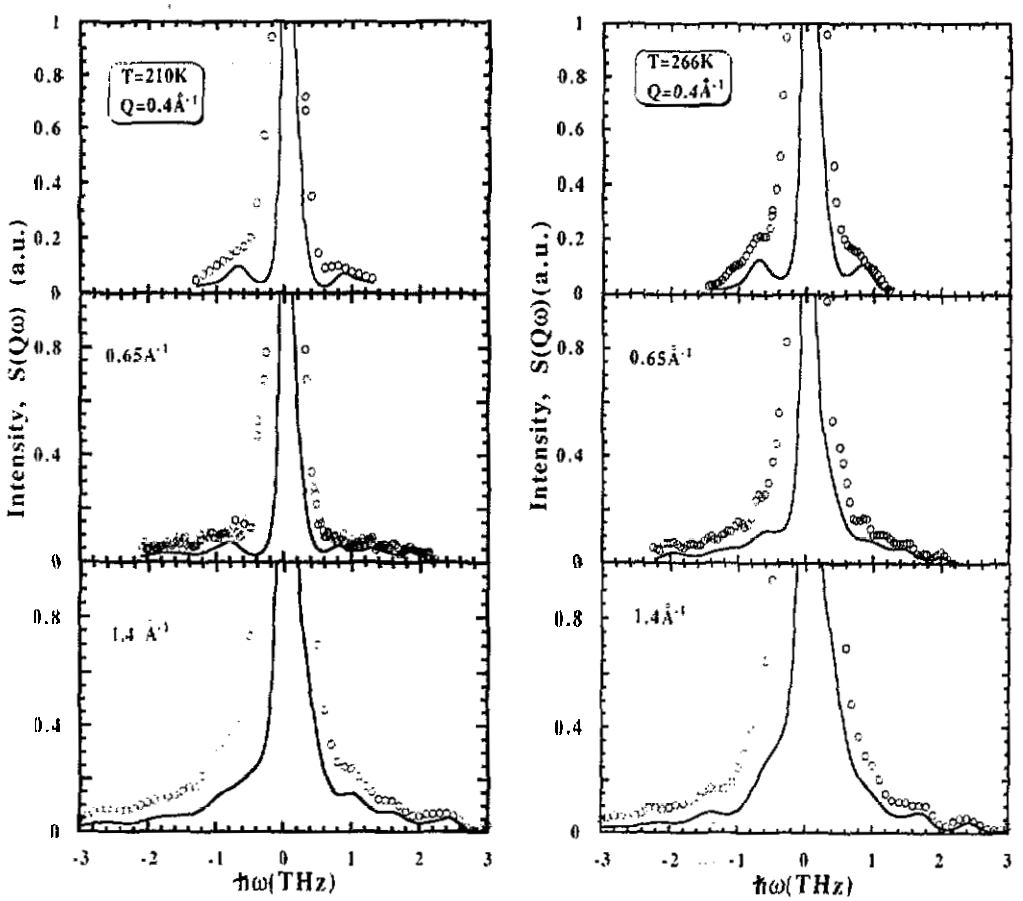

Figure 4. Reconstruction of the $S(Q, \omega)$ (unfolding) for several Q-values. (*a*) $T = 210$ K and (*b*) $T = 266$ K. Open circles represent experimental data and full curves are the deconvoluted spectra.

A set of deconvoluted spectra is shown in figure 4, where it can be seen that side peaks are clearly visible up to 0.7 $Å^{-1}$ for $T = 210$ K and up to 0.45 $Å^{-1}$ for $T = 266$ K.

4. Discussion

4.1. Crossover to the overdamped regime

The simplified viscoelastic approximation used to analyse the present data predicts the appearance of well resolved inelastic peaks located at frequencies

$$\omega_m = \tfrac{1}{3}\{2\omega_l^2 - \tau^{-2} + [\omega_l^4 + \tau^{-4} - 2\tau^{-2}(2\omega_l^2 - 3\omega_0^2)]^{1/2}\}^{1/2} \tag{8}$$

when

$$3\omega_0^2 - \omega_l^2 > 0. \tag{9}$$

In order to test the approximations involved (i.e. a single relaxation time for the

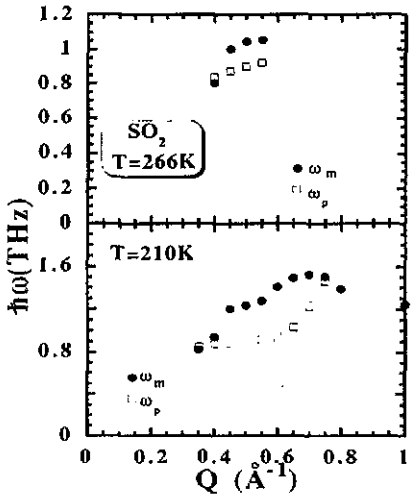

Figure 5. Dependence on Q of the peak maxima. Full circles are the values computed from the fitted parameters using the viscoelastic approximation (equation (8)). Open squares are estimated positions of the maxima of the deconvoluted $S(Q, \omega)$. Upper frame: $T = 266$ K; lower frame: $T = 210$ K.

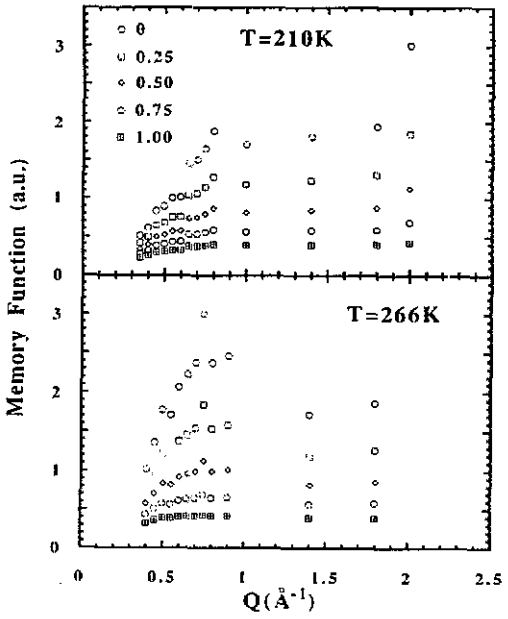

Figure 6. Dependence on wavevector of the memory function for several time values. Upper frame: $T = 210$ K; lower frame, $T = 266$ K.

decay of the memory function), we have compared the ω_m frequencies computed from the fitted parameters with the positions p of the maxima of the sidepeaks in the unfolded spectra. The results are displayed in figure 5 for both temperatures. Several remarks are in order regarding the graphs displayed in figure 5. First and foremost, the crossover to the overdamped regime predicted by the viscoelastic approach occurs at $Q = 0.55$ Å^{-1} at $T = 266$ K and at $Q = 1.0$ Å^{-1} for $T = 210$ K. The crossover occurs at the same momentum-transfer value in the high-temperature case, but an apparent discrepancy is found between the two values in the spectra taken at 210 K. Although it seems clear upon inspection of figure 4 that above $Q = 0.6$ Å^{-1} the identification of the sidepeaks in the deconvolved spectra becomes rather difficult (estimated using a first derivative), and, on the other hand, the estimated error in the peak position becomes quite large, inspection of the two graphs reveals some systematic differences between the peak frequencies estimated by the two methods. An analogous effect may be noted if one compares the experimental and molecular dynamics results for liquid Rb with the predictions made by the viscoelastic theory [1], and it can be partly attributed to the oversimplification caused by the use of a single-exponential approach for the memory function.

4.2. Longitudinal viscosity and associated memory function

As described in the previous section, the dependence on Q of the longitudinal viscosity can be easily described using equation (5), in terms of its $Q = 0$ value and a critical

Q-value defining the crossover to the non-propagating regime. However, the fitted values for Q_c are significantly larger than both those obtained from the use of the viscoelastic model and those obtained from inspection of the unfolded spectra. In order to explore the reasons for such discrepancy, the free-streaming value for the Q-dependent longitudinal viscosity was computed for $Q = 20\ \text{Å}^{-1}$ (the reciprocal coherence length). The free streaming values computed from the calculated thermal velocities were $\eta_l^{\text{free}} = 0.019 \times 10^{-3}$ and $0.016 \times 10^{-3}\ \text{N s m}^{-2}$ for $T = 210\ \text{K}$ and $T = 266\ \text{K}$, respectively. On the other hand, the values computed from the fitted parameters are about two orders of magnitude smaller than the free-streaming limits, thus indicating the need for taking into account a more slowly decaying component in order to satisfy this free-particle property.

The memory function associated with the longitudinal viscosity is simply [1]

$$m_l(Q, t) = (\omega_l^2 - \omega_0^2) \exp(-t/\tau) \tag{10}$$

and the shape of the functions for several values is depicted in figure 6.

Although this simplified form for the memory function does not reproduce the correct high-Q limit, it is able to take into account the most relevant features of the collective response of the liquid in terms of a small number of parameters, which makes the approximation presented here a useful tool for analysing experimental data. Recent analysis of molecular dynamics data on a molecular liquid [17] has shown that the model used in this work satisfactorily reproduces both the simulated spectra and the 'dispersion relation' obtained.

There is an obvious choice as regards reconciling the discrepancies found in the present treatment: either (i) to relax the condition given by equation (2) for the calculation of the relaxation time; or (ii) to use a two-relaxation-times model for the memory function following the same lines as those used to analyse molecular dynamics results [18, 19]. Neither of these approaches was attempted since in both cases they lead to an increase in the number of parameters to be fitted to the experimental intensities and, therefore, to a more unstable parameter estimation problem.

4.3. Spatial dispersion of the excitation

The dispersion behaviour of the ω_0-moment turns out to be quite close to that of a simple atomic system up to a Q-value of about $1.0\ \text{Å}^{-1}$. For larger momentum transfers the rather broad shape located within the range from 1.0 to $1.8\ \text{Å}^{-1}$ cannot be adequately reproduced with such a simple model. This should be attributed to the presence of strong orientational correlations, clearly evident in the previous neutron diffraction study, which make the approximation of weak anisotropy employed to derive equations (7*b*) and (7*c*) break down at this length scale. Up to the present moment no other workable model has existed to extend the range of validity towards larger Q-values, and therefore the only method available for full analysis of the dispersion behaviour is the computer molecular dynamics simulation of such a system.

Finally, it was noticed from the outset that the observed intensities were explainable in terms of the presence of collective excitations of 'acoustical' nature. Therefore, no signature was observed regarding the collective oscillations in the polarization function, as recently envisaged by Chandra and Bagchi [3]. The present study thus corroborates evidence for the extreme difficulty of observing such excitations, possibly due to the very large damping associated with this collective excitation. However, sulphur dioxide

constitutes an ideal candidate for the search for such excitations since its relatively large dielectric and rotational constants are the prerequisites indicated in [3] as necessary for the detection of this kind of excitation.

On the other hand, an estimation of the dipolaron frequency as well as the condition for the existence of this kind of longitudinal oscillations can be carried out along the lines suggested by Madden and Kivelson [20]. From [20], it can be seen that the dipolaron frequency is given by

$$\omega_d = \omega_s(2\varepsilon(0) + \varepsilon(\infty)/3g^s)^{1/2}/\varepsilon(\infty) \tag{11}$$

where ω_s corresponds to the free (inertial) reorientation time computed from the average molecular moment of inertia, $\varepsilon(0, \infty)$ are the zero- and infinite-frequency permittivities and were set to values of the static dielectric constant ($\varepsilon(0)$) and to the square of the optical index of refraction ($\varepsilon(\infty)$), and g^s is the Kirkwood factor obtainable from the measured $g(r)$ distribution functions [20]. The value computed with the parameters [21] $\varepsilon(0) = 17.6$, $\varepsilon(\infty) = 1.99$, $g^s = 1.4$, and $\omega_s = 0.517\ \text{ps}^{-1}$ gives a frequency of 1.52 THz for this collective excitation.

The condition for the existence of 'dipolaron' oscillations can be written in a simplified form as

$$\varepsilon(0)\varepsilon(\infty) \geqslant \omega_s^2\tau_s\tau_D/4 \tag{12}$$

where τ_D corresponds to the Debye rotational diffusion correlation time and was set to the value of 0.41 ps estimated in section 2 for $T = 266$ K, and τ_s can be computed from the available values using equation (10.8*a*) of [20] which gives a value of 0.21 ps. The first term of the inequality thus becomes 35.044, which is obviously larger than 0.044 corresponding to the second term, thus making the case of liquid SO_2 an extremely favourable case for the study of the phenomena referred to.

Such a simple calculation would indicate the presence of this excitation in the far-infrared spectra or in the density of states measured in a neutron experiment. Its not being observed in the present set of experiments may be attributed to the rather different length scales that correspond to neutron and optical probes. It is then clear that future far-infrared and low-frequency neutron experiments are necessary to test the predictions given above.

5. Conclusions

The inelastic neutron scattering spectrum of liquid sulphur dioxide exhibits some distinctive characteristics compared with those observed in other molecular liquids [22, 23]. First of all, the inelastic intensities arising from short-wavelength density oscillations are clearly visible without our having to have recourse to deconvolution procedures, as done in the past with some other molecular liquids [6, 7]. On the other hand, the spatial dispersion of the excitation shows characteristics rather different to the ones recently observed in a hydrogen-bonded liquid under similar thermodynamic conditions. In particular, the rather flat shape of the dispersion curves in the region $0.9 < Q < 1.4\ \text{Å}^{-1}$ is in sharp contrast with the features observed in liquid methanol [6, 7, 17], which have been reproduced in a recent molecular dynamics simulation [17]. It is obviously difficult to assess the nature of such differences although something can be gained by noticing that the relaxation times in this liquid are consistently shorter than in methanol. This could be interpreted as an indication of longer excitation lifetimes in methanol at length

scales comparable with the interparticle separation; that is, the solid-like character of the hydrogen bond manifests itself in this range of momentum transfers.

A neutron diffraction experiment [4] has shown that the strong orientational correlations found in the liquid phase indicate the persistence of some structural memory from the solid phase. The only available lattice dynamical calculation [24] has shown that most of the relevant interactions giving rise to phonon dispersion are located within a sphere of 6.2 Å, which in the liquid phase corresponds to the first minimum in the $g(r)$ pair correlation function. A recent Monte Carlo calculation [25] carried out using the same potential function as the one employed for the lattice dynamics study has demonstrated that at this length scale the structural arrangements in the liquid that give rise to the fine structure in the $g(r)$ up to 7 Å resemble those encountered in the solid phase. Finally, it is worth mentioning that no model potential is available that is capable of reproducing the experimental $g(r)$ up to distances of about 10 Å, and therefore further progress will have to wait until more realistic potentials are developed.

As mentioned in previous sections, the model scattering law used to analyse the data could be improved in order to predict the correct free-particle limit as well as to extend its domain of validity towards regions of larger momentum transfer. A step towards this would be to develop a viscoelastic theory that includes the effect of the molecular shape in terms of the appropriate distribution function. Such a model would give rise to new correlation functions describing the effects of collective rotations and their coupling to density oscillations, which should take into account the small deviations from the correct asymptotic behaviour found in this work.

Acknowledgments

Dr P Chieux of the Institut Laue–Langevin and Professor F Batallán are gratefully acknowledged for the help given during the sample-handling steps. This work was supported in part by DGICYT grants PB86-0617-C02 and PB89-0037-C03.

References

[1] Hansen J P and McDonald I R 1986 *Theory of Simple Liquids* (New York: Academic) ch 12
[2] Lobo R, Robinson J E and Rodriguez S 1973 *J. Chem. Phys.* **59** 5922
Pollock E L and Adler B J 1981 *Phys. Rev. Lett.* **46** 950
[3] Chandra A and Bagchi B 1990 *J. Chem. Phys.* **92** 6833
[4] Alvarez M, Bermejo F J, Chieux P, Enciso E, García-Hernández M, García N and Alonso J 1989 *Mol. Phys.* **66** 397
[5] Blank H and Maier B (ed) 1988 *Guide to Neutron Research Facilities at the ILL, Grenoble, France*
[6] Bermejo F J, Batallán F, Martínez J L, García-Hernández M and Enciso E 1990 *J. Phys.: Condens. Matter* **2** 6659
[7] Bermejo F J, Batallán F, Enciso E, García-Hernández M, Alonso J and Martínez J L 1990 *Europhys. Lett.* **12** 129
[8] García-Hernández M *IN8 Applications Software* private communication
[9] *Programme Rescal* Institut Laue–Langevin software
See also
Dorner B 1972 *Acta Crystallogr.* A **28** 319
Cooper M J and Nathans R 1967 *Acta Crystallogr.* **23** 357
[10] Lovesey S W 1984 *Theory of Neutron Scattering from Condensed Matter* (Oxford: Oxford University Press) ch 6
[11] Sokolic F, Guissani Y and Guillot B 1985 *Mol. Phys.* **56** 239

[12] Wasylishen R E, McDonald J B and Friedrich J O 1984 *Can. J. Chem.* **62** 1181
[13] Hu C M and Zwanzig R 1974 *J. Chem. Phys.* **60** 4354
[14] Bermejo F J, Alvarez M, García-Hernández M, Mompeán F, White R P, Howells W S, Carlile C J and Enciso E 1991 *J. Phys.: Condens. Matter* **3** 851. This contains a study of the dynamics of liquid CCl_4 where the coherent effects are explicitly taken into account.
[15] Alley W E, Alder B J and Yip S 1983 *Phys. Rev.* A **27** 3174
[16] Bhatia A B and Singh R N 1985 *Phys. Rev.* B **31** 4751
[17] Alonso J, Bermejo F J, Martínez J L, García-Hernández M and Howells W S 1991 *J. Mol. Struct.* at press
[18] Rahman A 1974 *Phys. Rev.* A **9** 1667
[19] Levesque D, Verlet L and Kurkijarvi J 1973 *Phys. Rev.* A **7** 1690
[20] Madden P and Kivelson D 1984 *Advances in Chemical Physics* vol 56 (New York: Wiley) p 467
[21] *International Critical Tables* 1926 vol 1 (New York: McGraw-Hill)
[22] Data are available for water (see Bosi P *et al Lett. Nuovo Cimento* **21** 346), methanol (see [6] and [7]) and hydrogen (see Carneiro K *et al* 1973 *Phys. Rev. Lett.* **30** 481)
[23] Boon J P and Yip S 1982 *Molecular Hydrodynamics* (New York: McGraw-Hill)
[24] Rastogi A, Anderson A and Leech J W 1979 *Can. J. Phys.* **57** 2120
[25] Enciso E 1991 unpublished data
The simulation was performed at $T = 210$ K.